GAMMA RAYS FROM VARIOUS (C^{12}, X) REACTIONS

by

ERICH WILHELM DREYER

Vordiplom, Justus Liebig Universitat, Giessen, Germany, 1970

A MASTER'S THESIS

submitted in partial fulfillment of the

requirements for the degree

MASTER OF SCIENCE

Department of Physics

KANSAS STATE UNIVERSITY
Manhattan, Kansas

1973

Approved by:

James C. Legg
Major Professor

TABLE OF CONTENTS

ILLEGIBLE DOCUMENT

THE FOLLOWING DOCUMENT(S) IS OF POOR LEGIBILITY IN THE ORIGINAL

THIS IS THE BEST COPY AVAILABLE

1 INTRODUCTION

Up to now, no general model has been found to describe the structure of different nuclei and to predict the energy levels of an excited nucleus.

These levels are characterized by their excitation energy above the ground state, their spin, purity, lifetime and their decay scheme and multipole mixing of the gamma decay-radiation.

To study the energy levels, the nucleus must be in an excited state, which is usually achieved by the bombardment of a target with a beam of high energy particles, provided by an accelerator. The nuclear reaction then produces the desired nucleus in various excited states. Many experiments with proton or neutron beams have been done and several nuclear models have been developed to fit the data gained by these experiments.

A more recently introduced method uses heavy particles, for instance C^{12} or O^{16} (so-called heavy-ion beams), as projectiles. The nuclear reaction is more complex than p or n reactions, but this method has the ability to excite very high spin states in the residual nucleus. Together with coincidence methods and certain geometries for target and detectors, it is possible to find new, higher-energy levels and to determine their quantum numbers, which are used to test different model predictions.

The topic for this thesis was a survey of various targets X with a mass number A in the range of $20 \leq A \leq 40$ to observe possible reactions and to investigate the energy levels and their decay scheme of the residual isotope Y in an X (C^{12}, α) Y reaction.

Na^{23}, Si^{28}, S^{32}, Cl^{35}, Cl^{37} and K^{39} were used as targets. First, a number of alpha-gamma coincidence measurements were performed to find out if the wanted reaction took place and which energy levels were populated. Second, gamma-gamma coincidence measurements gave evidence about the decay scheme of the different excited states.

2 THEORY

2.1 Nuclear Reaction

The process involved when a beam of high energy particles hits a target may be described by the following notation:

1) $a + X \rightarrow Y + b$

X: target nucleus

Y: residual nucleus

a: projectile

b: outgoing particle or gamma quanta

Elastic and inelastic scattering, where Y and b are not different from X and a, shall be excluded. Then 1) is called a nuclear reaction. Its short form notation is:

2) X (a,b) Y

or

3) X (a,b γ) Y

when it shall be emphasized that also a gamma ray is observed.

There are some basic conditions for the nuclear reaction to take place with a large cross section:

4) $E_{CM} + Q > E_{Coul.}$ (Y + b)

where E_{CM} is the center of mass (CM) energy, calculated from the laboratory (Lab) energy of the projectile a by:

5) $$E_{CM} = \frac{M_X}{M_X + M_a} \times Ea_{Lab} \qquad (1)$$

and Q is the reaction Q -value:

6) $Q = C^2 (M_X + M_a - M_Y - M_b)$

C: velocity of light in vacuum

M_i: respective masses

The coulomb barrier energy is calculated by

7) $$E_{Coul}\ (Y + b) = \frac{Z_Y \times z_b \times e_o^2}{R}$$

e_o: electronic charge

Z, z: atomic numbers of heavy and light particle

R: nuclear radius of heavy particle

8) $$R \approx 1.4\ fm \sqrt[3]{A}$$

A: mass number of heavy particle

Also the CM energy of the reaction must be in the range (not necessarily greater because of the tunnel effect) of the coulomb barrier energy of X + a.

Table 1 shows target and residual nucleus, laboratory and center of mass energy of the projectiles, coulomb barrier energies and Q value for the X (C^{12}, α) Y reaction and in the last two columns the numbers for the reaction condition 4). C^{12} and O^{16} are included, because they were abundant in nearly all targets as impurities.

Table 1

Target X	Resid. Nucleus Y	Q Value	$E_{a_{Lab}}$	E_{CM}	E_{Coul} $(X + C^{12})$	$(Y + \alpha)$	$E_{CM} + Q$
C^{12}	Ne^{20}	4.62	24.0	12.0	15.3	7.58	16.62
O^{16}	Mg^{24}	6.77	24.0	13.7	19.6	8.7	20.47
Na^{23}	P^{31}	12.49	24.0	15.8	23.8	9.76	28.29
Si^{28}	Ar^{36}	6.32	24.0	16.8	28.4	10.04	23.12
S^{32}	Ca^{40}	6.4	24.0	17.5	31.5	11.37	23.9
Cl^{35}	Sc^{43}	4.7	24.0	17.9	32.0	17.56	22.6
Cl^{37}	Sc^{45}	6.87	24.0	18.1	32.0	12.56	24.99
K^{39}	V^{47}	5.8	24.0	18.3	34.5	13.33	24.1

Table 1 shows that for all the cited targets the X (C^{12}, α) Y reaction is energetically possible.

A nuclear reaction can be separated into different classes according to the lifetime of the intermediate state. The minimum lifetime would be about the time the projectile needs to traverse a distance similar to the dimensions of the target nucleus (ca 10^{-22} sec, (4) page 191). These are the direct reactions.

Sometimes this lifetime is considerably longer (up to 10^{-16} sec, (4)). The state is then called a compound state and it is said, that a compound nucleus is actually formed. The 'Bohr Compound Nucleus Assumption' ((2) page 340) says, that the decay of the compound nucleus is independent from its generation.

In heavy ion reactions normally one cannot determine if either a direct or a compound nucleus reaction takes place; in many cases it is probably a mixture of both processes. The intermediate state however, shall be called a compound state.

Equation 1) can be rewritten as:

9) $a + X \rightarrow (C)^* \rightarrow b + Y + \gamma$

where $(C)^*$ is the compound state which decays under emission of particle b to the residual nucleus Y, which, if it is in an excited state, decays by emitting gamma radiation.

A special mode of decay of a compound nucleus is called a channel. The compound state can only decay through a certain channel, if the CM energy of the compound nucleus is greater than the respective minimum seperation energy S_{Min}:

10) $S_{Min} = - c^2 \times (M_C - M_b - M_Y)$

In Table 2 minimum seperation energies, calculated from 10), are listed for alphas, protons, neutrons and deuterons for the different compound nuclei.

Table 2

Target	Compound Nucleus	Alpha	S_{Min} in MeV Proton	Neutron	C^{12}	Deuteron
C^{12}	Mg^{24}	9.32	11.69	16.53	13.93	16.14
O^{16}	Si^{28}	9.38	11.58	17.17	16.75	22.41
Na^{23}	Cl^{35}	7.00	6.37	17.63	19.49	15.56
Si^{28}	Ca^{40}	7.04	8.33	15.62	13.36	19.20
S^{32}	Ti^{44}	5.23	8.77	13.39	11.65	18.65
S^{34}	Ti^{46}	8.01	10.35	13.19	14.18	19.45
Cl^{35}	V^{47}	8.35	5.18	13.02	13.00	16.14
Cl^{37}	V^{49}	9.31	6.75	11.55	16.19	16.16
K^{39}	Mn^{51}	8.67	5.3	13.68	14.46	16.01

From Table 2 it can be seen, that S_{Min} for alphas and protons is, for all considered cases, lower than S_{Min} for C^{12}. Since the compound state is formed with bombardment of C^{12} particles, alpha and proton decay are always possible. The exit channel with the smallest S_{Min} is the most probable from the viewpoint of energy. Obviously this is alpha and proton decay.

The whole process of the nuclear reaction is sketched in Figure 1 for alpha decay.

THIS BOOK CONTAINS NUMEROUS PAGES WITH DIAGRAMS THAT ARE CROOKED COMPARED TO THE REST OF THE INFORMATION ON THE PAGE.

THIS IS AS RECEIVED FROM CUSTOMER.

Figure 1

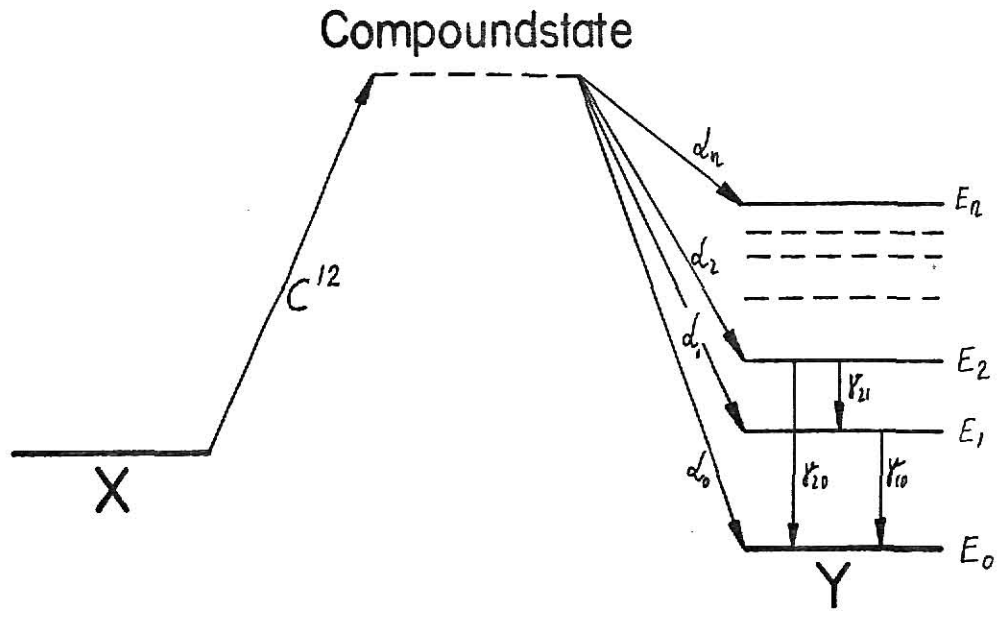

Figure 1 shows the different steps of the $X(C^{12}, \alpha\gamma)Y$ reaction. Energy levels are arbitrary.

The compound state is normally not a sharp state for heavy ion reactions, i.e., it has no definite angular momentum and energy. For the highest populated states with an excitation E_n in Y we can write the condition:

11) $$E_n \leq E_{\alpha_{0_{CM}}} - S_{Min}(\alpha)$$

Although proton decay has energetically about the same probability as alpha decay and $E_{Coul}(Y + b)$ in 4) is even lower for proton decay, alpha decay is predominant in these experiments because of angular momentum matching conditions. In many cases the angular momentum to be carried away by the outgoing particle is so high that its impact parameter would exceed the radius of the nucleus in the case of proton decay. Thus, decay by emission of heavier particles is favored.

2.2 Geometry

Assuming the conditions for the wanted nuclear reaction are fulfilled, then the measurable parameters, such as the nature of the outgoing elements b (gamma quant or what kind of particle), their energy, spatial distribution and simultaneous occurrence have to be related to the parameters specifying a certain energy level.

The height of an electronic pulse generated in a detector is proportional to the energy. The other parameters like spin, parity, lifetime, decay scheme and multipole mixing have to be deduced from this pulse height spectrum.

Naturally the geometric setup, i.e. the positioning of target and detectors relative to the beam axis, and the electronic setup, containing certain coincidence and energy selective conditions (windows), depend very much on which of the above cited parameters shall be determined. The electronic setup is described below.

The geometry chosen for the particle-gamma experiments was the one of Litherland and Ferguson (LF) No. II, described in (3), where emergent particles are detected in a small axially symmetric counter at zero degrees to the beam direction (forward direction), which is used as quantization or z-axis. Gamma quanta are counted with a second detector moving in a plane to the z-axis.

In the experiments performed the gamma detector was fixed at 90 degrees and angular correlations were not measured.

The advantage of the LF geometry No. II is, that there are certain restrictions on the parity and the magnetic quantum number of populated states of the residual nucleus Y. Considering the reaction

X (a,b) Y, we have for spin and parity conservation the result:

$$12)\quad \vec{J}_X + \vec{S}_a + \vec{l}_a = \vec{J}_Y + \vec{S}_b + \vec{l}_b$$

$$13)\quad \pi_X \times \pi_a \times \pi_{l_a} = \pi_Y \times \pi_b \times \pi_{l_b}$$

$\vec{J}$: spins of X, Y

$\vec{s}$: spins of a, b

$\vec{l}$: orbital momenta

π_i: respective parities

Considering the z components of the spin:

$$14)\quad J_{X_z} + S_{a_z} + l_{a_z} = J_{Y_z} + S_{b_z} + l_{b_z}$$

The LF geometry No. II causes l_{a_z} and l_{b_z} to be zero, because a and b are moving along the quantization axis. This results in the condition, that the z-component of a certain state of Y cannot be greater than the sum of the spins of X, a, and b.

In the experiments performed this condition was further simplified by using C^{12} for particle a and an alpha for b, both with spin zero, so that 14) reduces to:

$$15)\quad J_{X_z} = J_{Y_z}$$

If the target is an even-even nucleus with $J_X = 0$, then only substates of Y with magnetic quantum number m = 0 are populated. The angular mementum equation 12) reduces to:

$$16)\quad \vec{l}_a = \vec{J}_Y + \vec{l}_b$$

Since nuclei with ground-state spin zero have positive parity and orbital parities are equal to $(-)^l$ (natural parity), we find for the parity equation 13):

$$17)\quad \pi_{l_b} \times \pi_{J_Y} = \pi_{l_a}$$

The reaction amplitude under this special conditions includes a Clebsch Gordan coefficient of the form $\langle J_Y 0\ l_b 0 \mid l_a 0 \rangle$ which is zero unless J_Y has natural parity, i.e.:

$$\pi_Y = (-)^{1J} = 0+,\ 1-,\ 2+,\ 3-,\ \ldots$$

So in this case only alpha particles are detected which populate states in Y which possess natural parity.

Other general advantages of the LF geometry No. II are that, assuming an unpolarized beam, the populated states of Y are aligned, which means the two substates of one level with the same absolute value of m_i, are equally populated.

All of the above cited properties are independent of the mechanism of the nuclear reaction producing Y.

2.3 Spectra

The raw spectrum, i.e. just the amplified detector signal sorted by a multichannel analyzer, is often confusing, because in reality very many reactions, additional to the one we are interested in, occur together. Even if the target material should consist of only one isotope, there could be different outgoing particles such as alphas, protons, neutrons, etc. according to the different exit channels. But in reality there are often other isotopes of the target element abundant and also at least traces of other elements (for instance H_2O in crystalline elements).

To select only the reaction one is particularly interested in, coincidence methods are used. Only when a gamma and particle pulse occur in a defined time interval, are these pulses stored. This method can be energy selective. Windows are set over the alpha spectrum and the pulses of the gamma coincidence spectrum are sorted into different spectra, according to which energy window the alpha pulse lies. Of course, the windows can also be set over the gamma spectrum.

Two different ways to get windows were used in the experiments performed.

One method was the more direct method of using single channel analyzers in the electronic setup for the experiment, and the other was to take a two-parameter spectrum and sort this after the experiment with appropriate computer programs (PHA 2 programs).

The second method is better, because it leaves the possibility to decide after the experiments about the number and range of the different windows and to vary them any number of times.

In the right part of Figure 1 the residual nucleus Y and its energy levels, populated by α decay are seen.

The different groups of alpha particles are found as a sequence of peaks in the pulse amplitude spectrum of the alpha pulses. Figure 2 is an example.

Figure 2

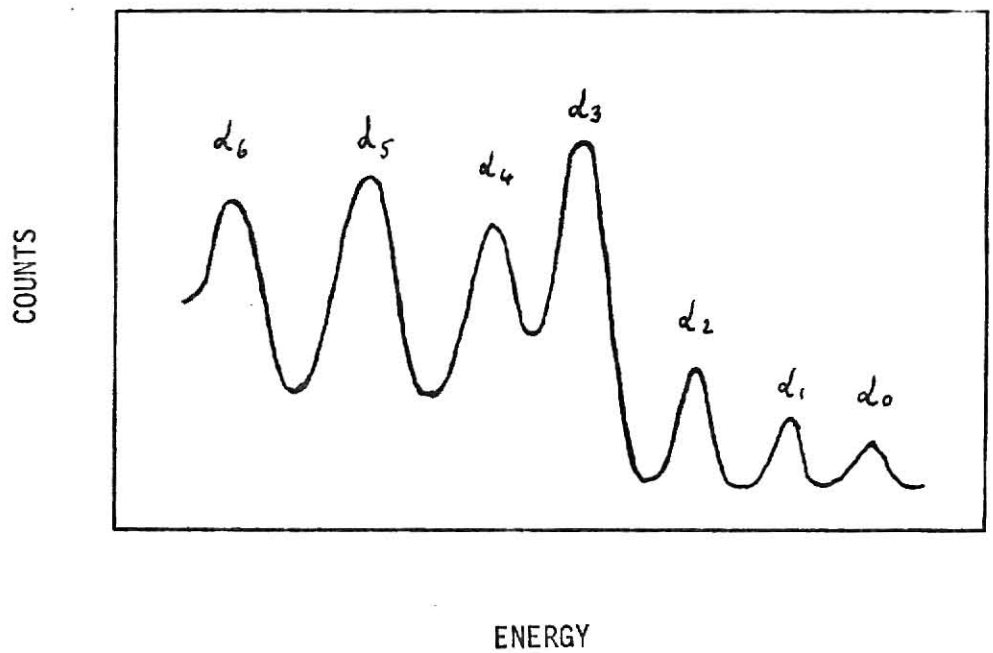

Figure 2. Schematic graph of a free alpha particle spectrum.

The peaks appear in the sequence of their indices from right to left, according to what energy levels in the residual nucleus are populated. α_0 represents the group of particles, which populate the ground state of Y and possess therefore the highest energy. Since they

occur without gamma-ray emission the α_0 peak vanishes in a gamma-alpha coincidence spectrum and is identified by this property. The energy of the 'ground state alphas' can be calculated for the different angles by reaction kinematics ((5) page 140).

Table 3 shows the energies of ground state alphas at 0° for the isotopes of interest for this thesis, at various beam energies.

Table 3

Target	E_{aLab}	$E_{\alpha oLab}$
C^{12}	24/24.5/26	26.38/26.82/28.13
O^{16}	24/24.5/26	29.19/29.65/31.01
Na^{23}	24	35.68
Si^{28}	24.5/26	29.74/31.15
S^{32}/S^{34}	24	29.47/30.87
Cl^{35}/Cl^{37}	24	27.77/30.07
K^{39}/K^{41}	24	28.96/30.69

If two different isotopes are abundant in one target and both are excited to alpha decay, the position of their peaks in the spectrum depends on the energy-difference of the respective E_{α_0} values. A frequently occurring case is the abundance of O^{16} and C^{12} in targets; therefore they are listed in the preceding tables. The O^{16} and C^{12} ground state alphas are separated by 2.82 MeV for a 24 MeV C^{12} beam, when detected at zero degrees.

It is difficult to calibrate an alpha spectrum when the thickness of the different targets is not known, or when an absorber foil in front of the detector is used, since the stopping power of heavy ions is not a linear function of the particle energy. Besides, the resolution of Si-particle detectors is not as good as the one for Ge(Li) gamma ray detectors, and alpha particle sources for calibration are not available in the needed range of 30 MeV (Table 3).

For gamma ray calibration we do not have these difficulties. Convenient sources like Co^{57} (0.1219 MeV), Na^{22} (0.511 MeV), and Y^{88} (1.836 MeV), which lie in the range of the first energy levels in our experiments, are available.

The gamma spectrum does not show the different energy levels in the sequence they are labeled in Figure 1, but depending on their energy. Calibrations as good as 0.5% are achievable.

3 EXPERIMENTAL SETUP

3.1 Accelerator, Detectors, and Electronics

The experiments for this thesis were performed with a C^{12} beam, charge state 4+ and 5+, at 24.0, 24.5 and 26 and 31.2 MeV, from the 6 MV Tandem Van de Graaff Accelerator at Kansas State University in Manhattan.

The spectra were taken and analyzed with Ortec and Canberra electronics and a Digital Equipment Corporation PDP-15 Computer with plotter. Software programs for storing single and dual parameter spectra and for manipulating, printing and plotting spectra were available.

Two Ge(Li) detectors, one with 3% and the other with 6% efficiency and about 2000 to 2200 Volt bias, and one Na I detector with a 3" x 3" crystal at 1050 Volt bias were used to take the different gamma spectra.

Particles were detected with a silicon surface barrier detector with 35 keV resolution for alpha particles and 300 μm depletion depth.

3.2 Targets, Target Chamber and Beam

The target elements used in the performed experiments were all in the range of: $20 \leq A \leq 40$ and were chosen for the following properties: The target substance should consist of one, or a chemical compound of two stable elements. Each element should consist mainly of one isotope and the intrinsic ground state spin should be low.

The first series of alpha-gamma coincidence experiments were performed with thin targets, of about 100-200 $\mu g/cm^2$ thickness. Substances were: NaCl for the Na^{23} and Cl^{35} target, enriched SiO_2 for the Si^{28} target, polymorphic sulfur for the S^{32} target, and KJ for the K^{39} target.

The Si target was a thin foil on formvar, while the other target materials were evaporated onto 10^{-2} mm (0.0004") gold foil. The gold foil targets show good mechanical stability and stop the beam. The stopping power for totally stripped C^{12} is 35.8×10^3 MeV/cm at 24 MeV and for alpha particles it is 1.84×10^3 MeV/cm at 30 MeV. The gold foil broadens the peaks of the alpha spectrum, but it keeps heavy particles from reacting the Si detector and is a good heat conductor.

For the gamma-gamma coincidence experiments (X (C^{12}, $\gamma\gamma$) Y) two ca. 1 mm thick targets of NaBr and $BaCl_2$ were used. This was done to separate the reactions from Cl and Na. The charge state of the carbon beam was changed from 4+ to 5+ to provide a higher beam energy of 31.2 MeV. The second member of each compound, Br^{80} with an atomic number Z = 35 and B^{138} with Z = 56 have coulomb barriers of 50.23 MeV and 67.11 MeV for a C^{12} beam and should not show any reaction.

The target chamber used for the experiments for the thin targets is sketched in Figure 3. A collimator shapes the beam when it is entering the target chamber from the beamline. Three interchangeable targets are mounted, one above the other, on the target holder, which is turned so that the targets have an angle of ca. 45° to the beam direction. This keeps the gamma rays, which are detected with a Ge(Li) detector under 90°, from interactions with the target frame.

A Si surface barrier detector, mounted inside the chamber, measures the particles in beam direction at zero degrees. Before entering the detector the particles have to pass through a 10^{-2} mm gold foil which stops the remaining C^{12} beam and a permanent magnet, which filters electrons and positrons out.

A C^{12} beam in the charge state 4+ of about 150 nA was chosen for the gamma-alpha experiments. For the gamma-gamma coincidence experiments the 5+ charge state was used in order to provide higher beam energy. Since the beam was entirely stopped in the thick targets and the reaction cross section increased at these higher energies, the low beam current of ca. 1.5 nA ensured a sufficient counting rate.

Further experiments shall use beams such as: C^{13}, N^{14}, O^{16}, O^{18} and F^{19}. The beam energy was selected by the analyzing magnet, whose magnetic field was measured by nuclear spin resonance methods. A computer program to calculate the terminal voltage of the accelerator and the frequency for the resonance fluxmeter for different beams and energies was available.

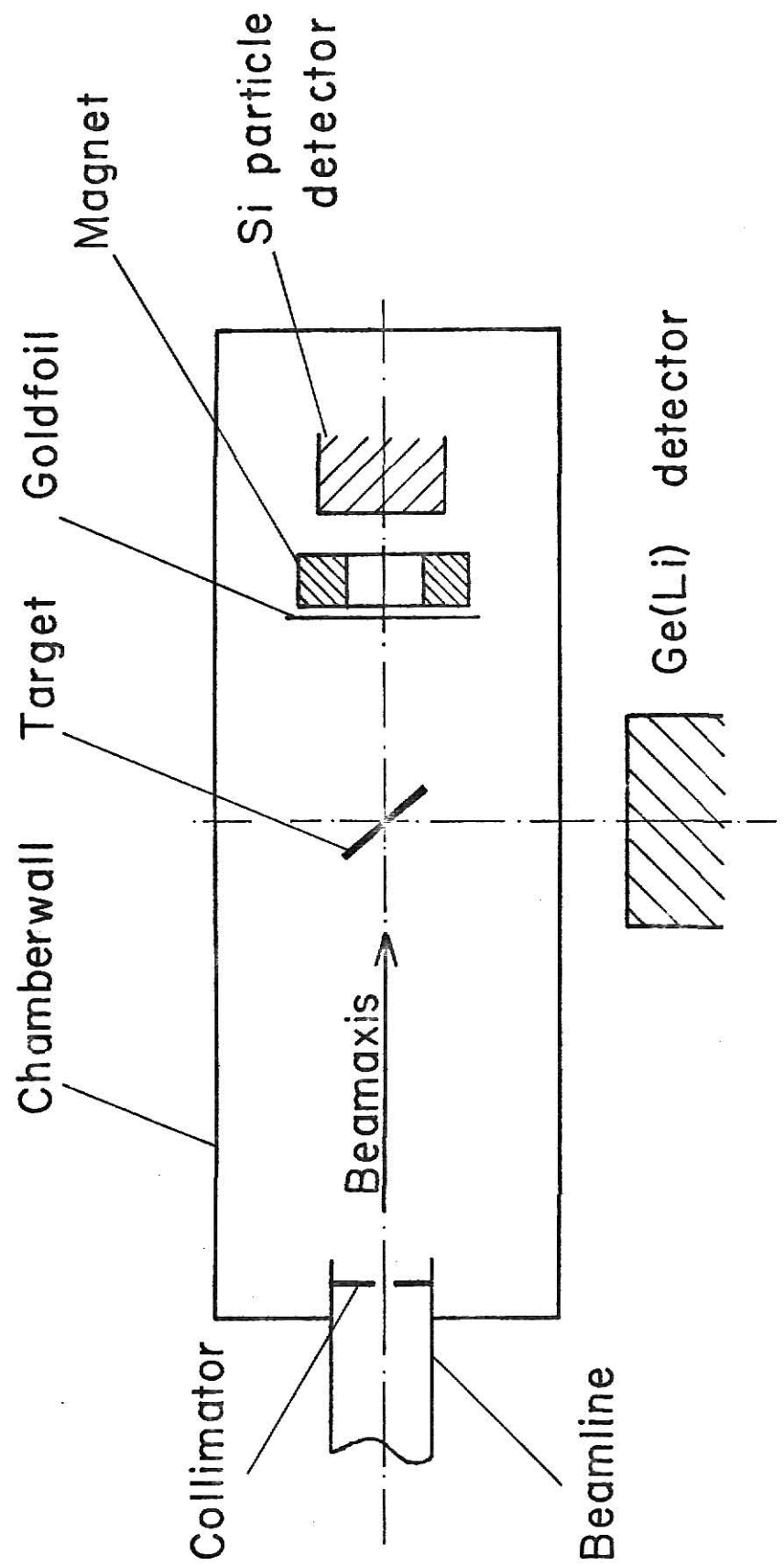

FIGURE 3 Targetchamber , seen from above.

3.3 Electronic Setup

The electronic setup was built with standard block elements for nuclear spectroscopy. It changed slightly during the experiments, but the general principle remained the same: two fast, preamplified timing pulses from the different detectors were used with a time-to-amplitude converter to obtain a fast coincidence signal, which by means of single channel analyser, logic shaper and delay, and overlap coincidence stages were used for the different coincidence signals for a mixer router and three analog to digital converters. Two of the ADC's had direct connections to the PDP 15 computer. The data was supervised during the experiment by an oscilloscope and stored on magnetic tapes for analysis.

4 RESULTS

4.1 Reactions with Sulfur, Silicon and Potassium

For the S, Si, and K target no evidence for a $X(C^{12}, \alpha)Y$ reaction was found at 24 MeV. The gamma spectra taken showed strong lines from Mg^{24}, Ne^{20} and Na^{23} resulting from impurities of O^{16} and C^{12} leading to the reactions:

$O^{16}(C^{12},\alpha)\ Mg^{24}$, $C^{12}(C^{12},\alpha)\ Ne^{20}$, $C^{12}(C^{12},p)\ Na^{23}$, and $C^{12}(C^{12},n)\ Mg^{23}$

All strong peaks in the particle spectra were identified as coming either from Mg^{24} (up to 10.9 MeV) or Ne^{20} (up to 7.23 MeV). Only states with natural parity were observed as long as particles were detected at zero degrees in agreement with the theory in Chapter 2.2.

The targets were intact after the experiment except the S target, where the heat provided by the beam had caused the sulfur to evaporate. This experiment should be repeated with a thin gold layer over the sulfur, to prevent evaporation.

4.2 Reactions with Sodium

The NaCl target showed a strong cross section for the $X(C^{12}, \alpha)Y$ reaction. Free, coincidence, and gated spectrum were taken for both, gamma rays and particles. The beam used was C^{12} at 24 MeV and 4+ charge state. Figure 4 shows the gamma spectrum from a Ge(Li) detector in coincidence with particles; all peaks identified with numbers result from P^{31}, or as found out later from P^{30}.

The different particle spectra could not be used for identification, they showed a strong continuum, topped with small peaks from Mg^{24} and Ne^{20} resulting from target impurities. This continuum, which was suspected to result from a three body breakup, will be explained later to be connected with the occurrence of P^{30}.

To exclude any contributions from chlori e and to find out about the decay scheme, a second gamma-gamma coincidence experiment with a thick NaBr target was performed. Since a test spectrum showed an increase of the wanted reaction and a decrease of reaction from impurities at higher beam energies, the charge state was switched to 5+ which allowed a maximum beam energy of 31.2 MeV.

A two parameter spectrum with pulses from a Ge(Li) detector along the horizontal axis and pulses from a Na I detector along the vertical axis was taken. Figure 5 shows the summation over the vertical axis; a total gamma coincidence spectrum from the Ge(Li) detector. The peaks marked by numbers are the same as listed under Figure 4. Their energies are consistent with data from P. M. Endt and C. van der Leun (8), which were used for all the following spectra and level

schemes. The 0.511 MeV annihilation line was so strong, that it caused a channel overflow of the ADC. The two lines from Na^{23} (0.439 and 0.627 MeV) and the Ne^{20} line (1.63 MeV) result from reactions with carbon and are probably due to implantations of beam particles in the target.

Windows were set over the 0.709 MeV line and the peaks 1, 2, and 4. In this way four vertical coincidence spectra (Figures 6, 8, 10, and 12) from the NaI detector were gained, each showing the gamma rays occuring in the same decay cascade as the respective coincidence peak. The channel compression used was 4, which explains the relatively narrow appearance of the peaks.

A closer look at the spectrum in Figure 5 showed, that the 0.709 and the 0.964 MeV line probably did not originate from transitions in P^{31} but in P^{30}, giving evidence for a successive neutron decay of P^{31}.

The argument for this assumption is that both lines are very sharp, which indicates that they originate from transitions between low-lying states. In P^{31} there is no such transition with a 0.709 gamma ray, and the 0.968 MeV gamma ray from the transition of the second to the first excited state (2.234 to 1.661 MeV) has only a branching ratio of less than 0.8% compared to more than 99% for the ground state transition of the 2.234 MeV level (8).

Figure 7 shows the part of the level diagram of P^{30} which is of interest for this thesis. The second excited state is at 0.709 MeV and a 0.964 MeV transition occurs between the 2.937 MeV and the 1.976

MeV level. The additional emitted neutron of the decay $P^{31} \rightarrow n + P^{30}$ explains the observed continuum of the particle spectrum for the NaCl target. Figure 7 shows more gamma rays at similar energies to those expected from the decay of P^{31}. These are at 1.267, 1.976 and 2.254 MeV, compared to 1.266, 1.957 and 2.234 MeV from P^{31} (Figures 7, 9, and 11). Since the resolution of the Ge(Li) detector was only about 10 keV FWHM for the 1.332 MeV line in Co^{60} and the peaks in Figure 5 show additional Doppler broadening, it was not possible to separate directly between contributions from P^{31} and P^{30} to the peaks 1, 2, and 4. In fact the spectra in Figures 8, 10, and 12 are mixtures of gamma rays from two different cascades, one in P^{31} and the other in P^{30}, which both happen to possess gamma rays of nearly the same energy, which could not be resolved any more. Figure 6 is composed of gamma rays from P^{30} only. For each of the coincidence spectra, the origin of the gamma rays is given on the successive page by part of the decay scheme of P^{30} and P^{31}.

It can be concluded, that sodium is an interesting target for a heavy ion reaction with C^{12} to study excited states of P^{31} and P^{30}.

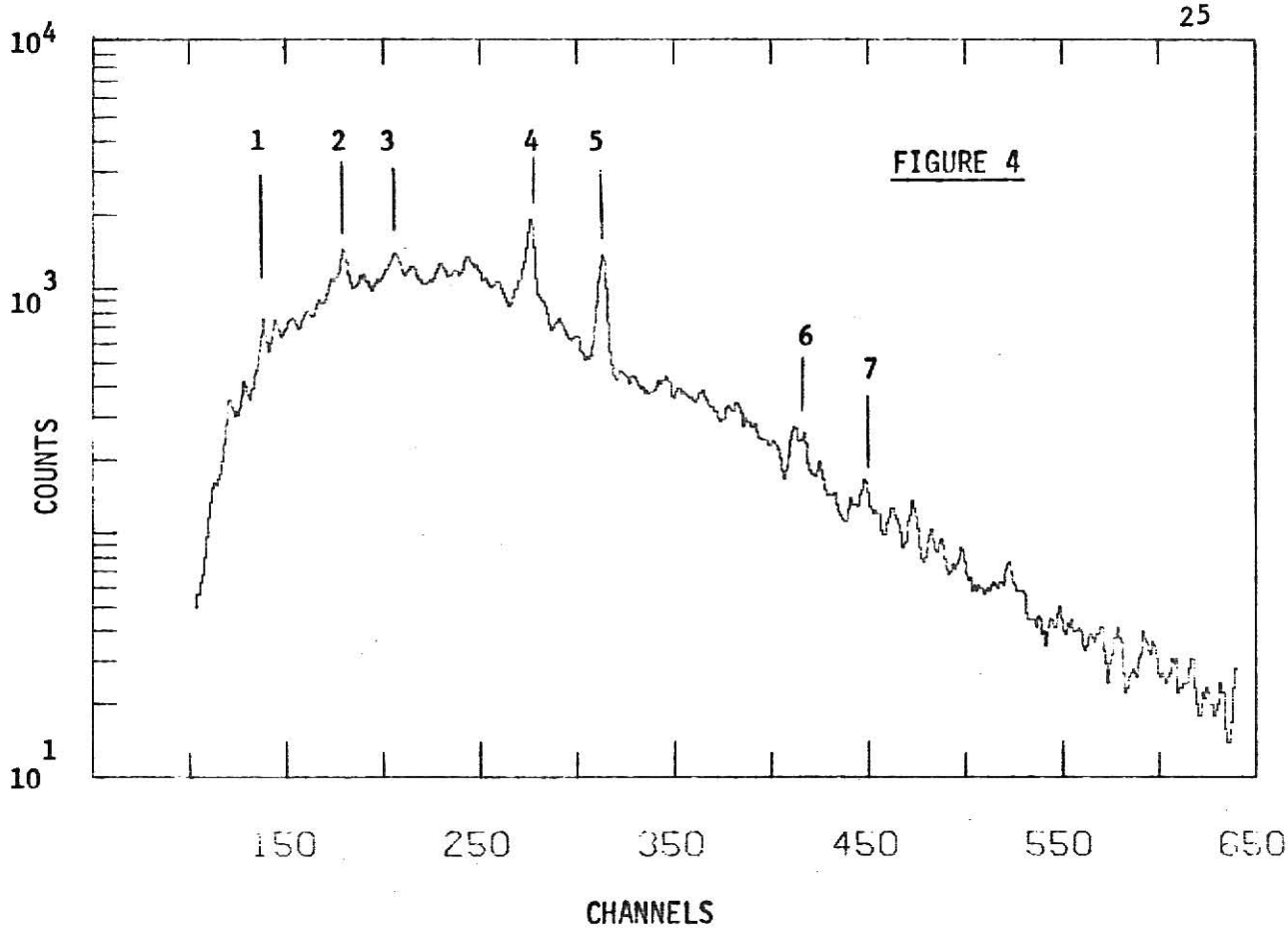

Figure 4 Gamma ray spectrum in coincidence with particles from the NaCl target taken with a Ge(Li) detector .

Identification of peaks :

No.	Energy in MeV	Isotope
1	0.968 /0.964	P^{31} / P^{30}
2	1.266 / 1.267	" / "
3	1.455	"
4	1.957 / 1.976	P^{31} / "
5	2.234 / 2.254	" / "
6	2.924 ; 2.994 / 2.937	" / "
7	3.165	"

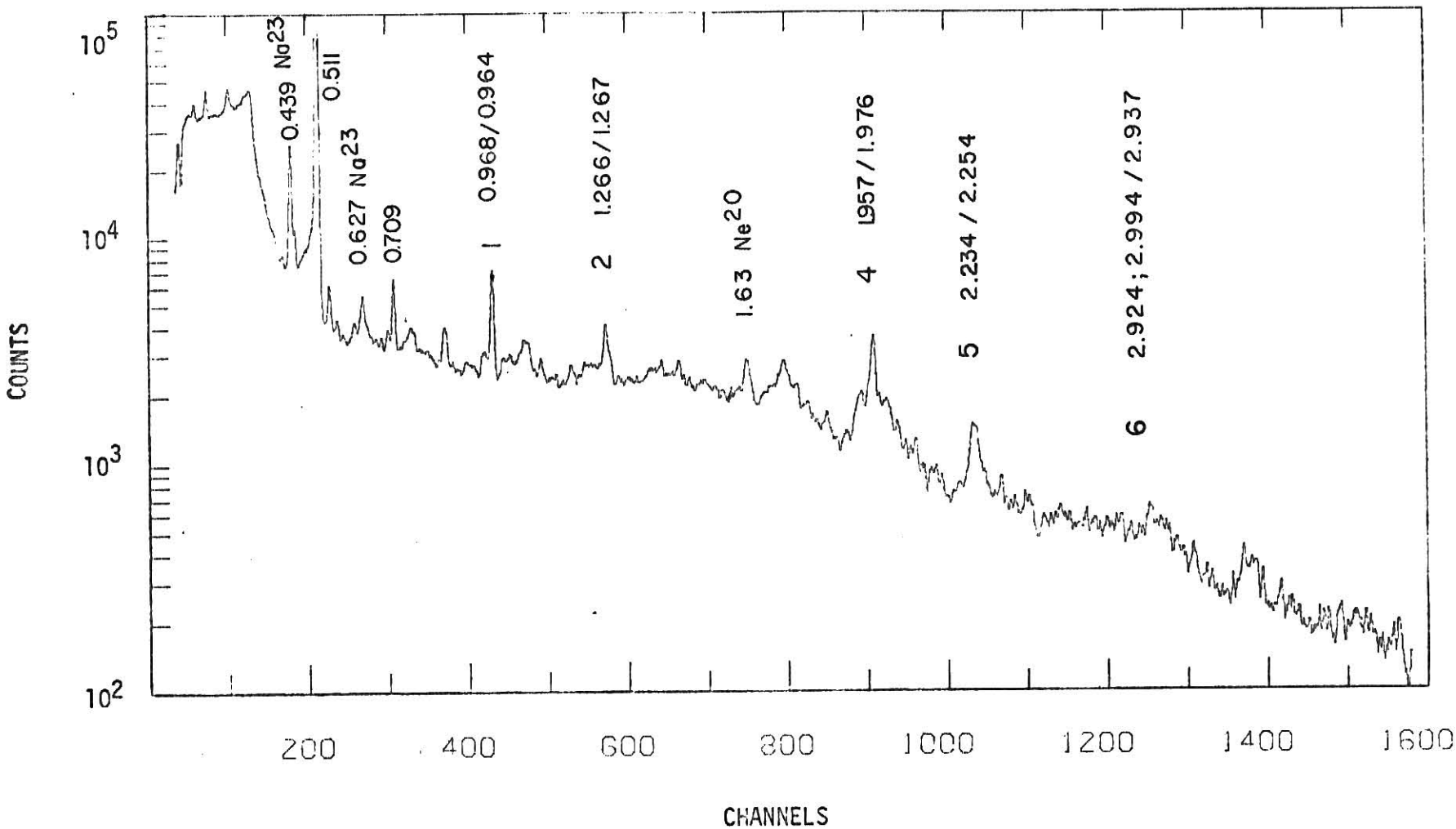

FIGURE 5 Total gamma ray coincidence spectrum from NaBr target. Taken with Ge(Li) detector.

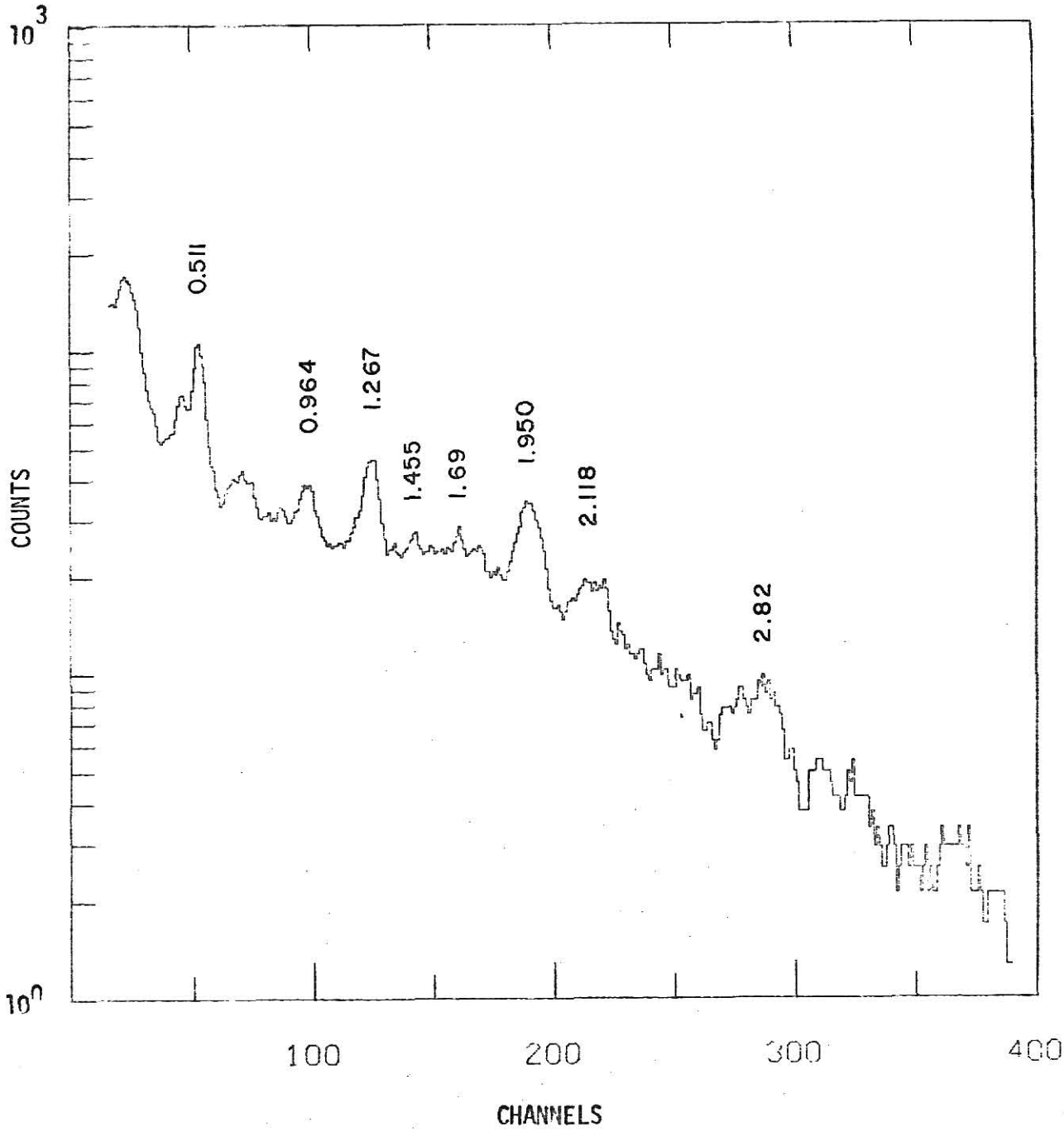

FIGURE 6

Figure 6 shows the coincidence spectrum of the 0.709 MeV gamma ray of P^{30} taken with a Na I detector.

FIGURE 7

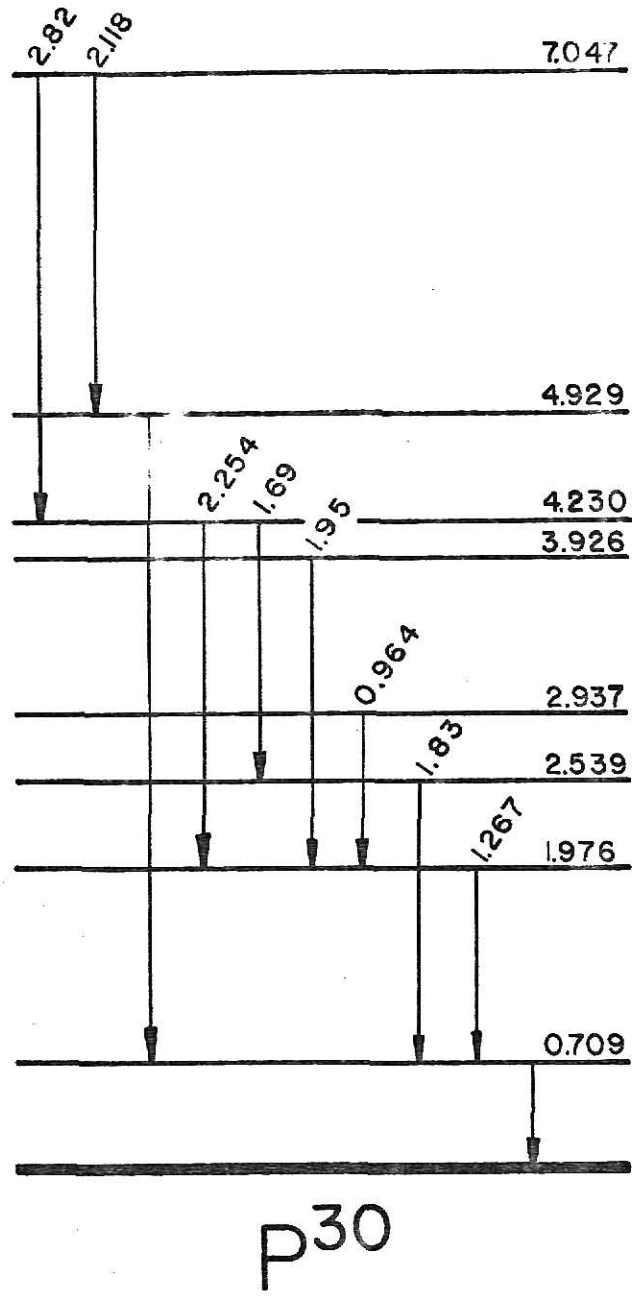

Figure 7 shows a part of the decay scheme of P^{30}. It is deduced from Figure 6 and reference (8).

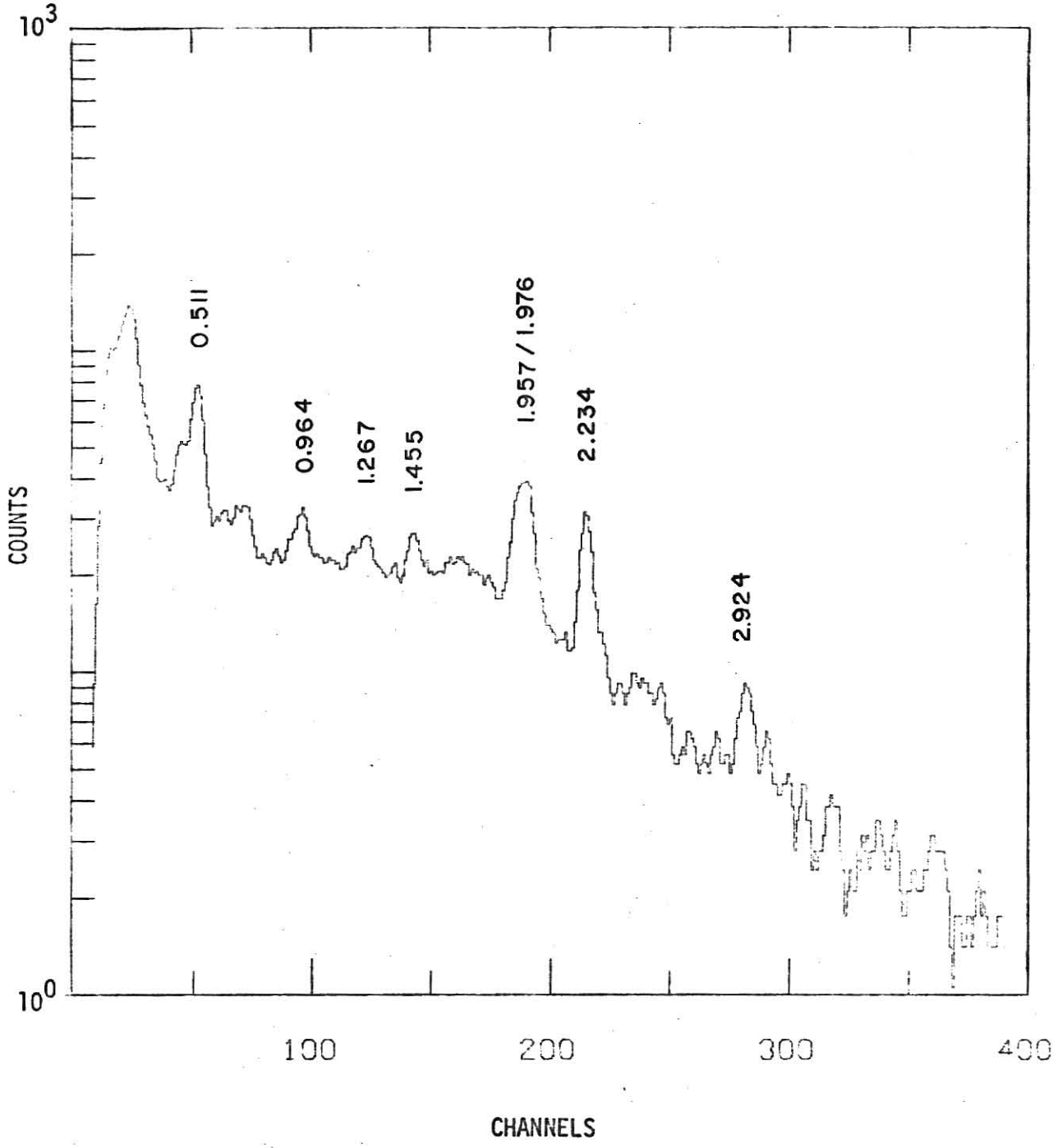

FIGURE 8

Figure 8 shows the coincidence spectrum of the 0.968 MeV transition from P^{31} and the 0.964 MeV transition from p^{30} taken with a NaI detector.

FIGURE 9

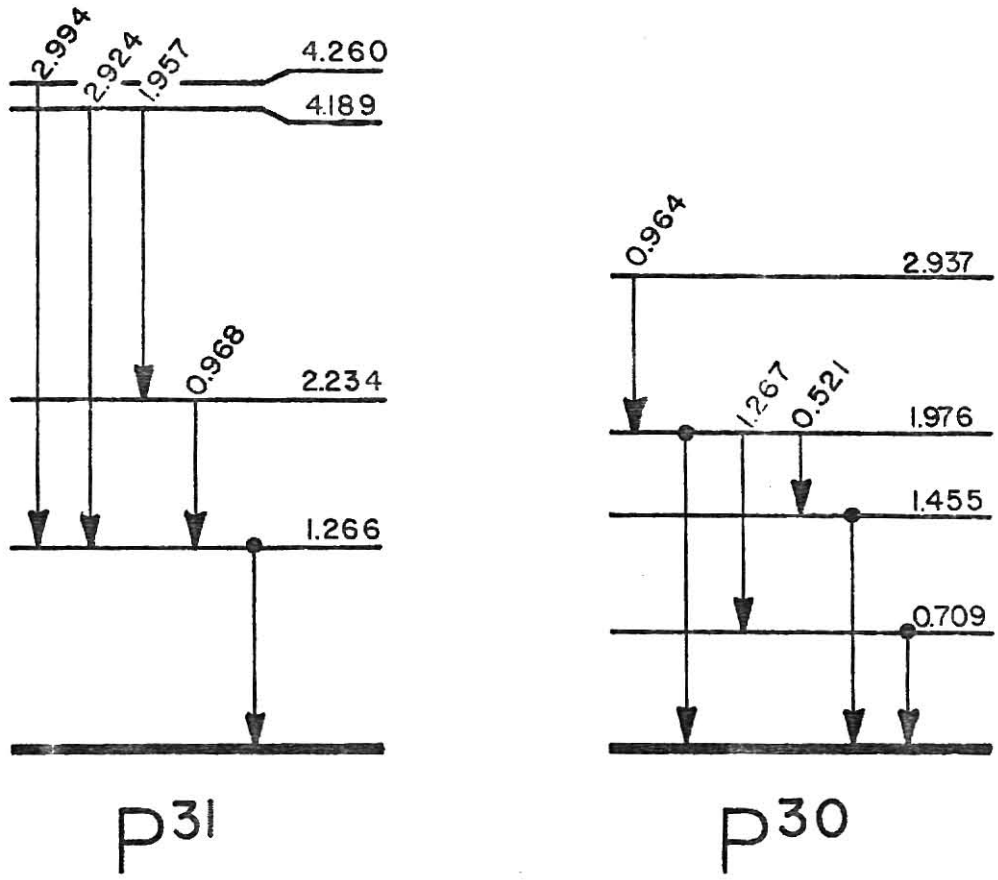

Figure 9 shows the parts of the decay schemes of P^{31} and P^{30} which contribute to the coincidence spectrum in Figure 8. The 0.968 MeV transition in P^{31} has a branching ratio of less than o.8%. Most of the peaks in Figure 8 come from P^{30} or random coincidences.

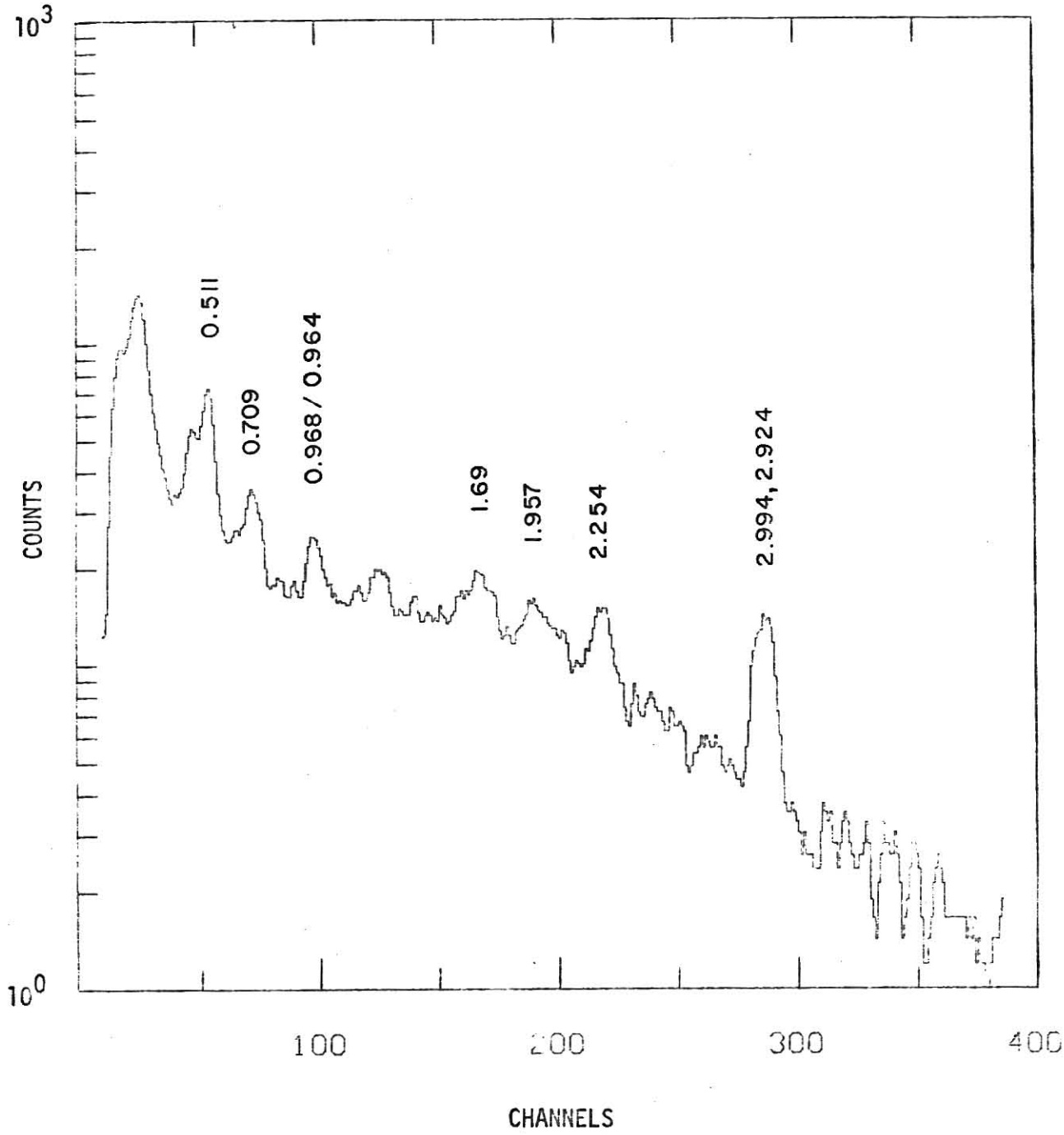

FIGURE 10

Figure 10 shows the gamma rays in coincidence with the 1.266 MeV first excited state in P^{31} and the 1.267 MeV transition in p^{30}. The spectrum was taken with a NaI detector.

FIGURE 11

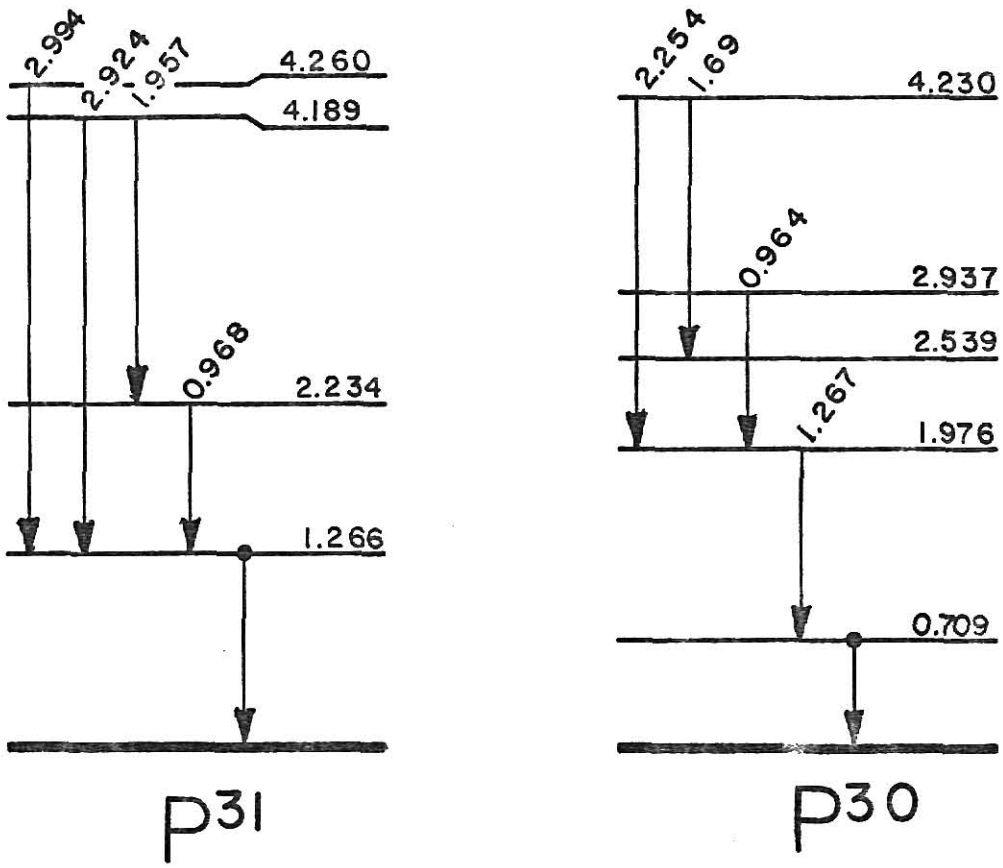

Figure 11 shows the parts of the level diagrams and the transitions of P^{31} and P^{30} which contribute to the spectrum in Figure 10.

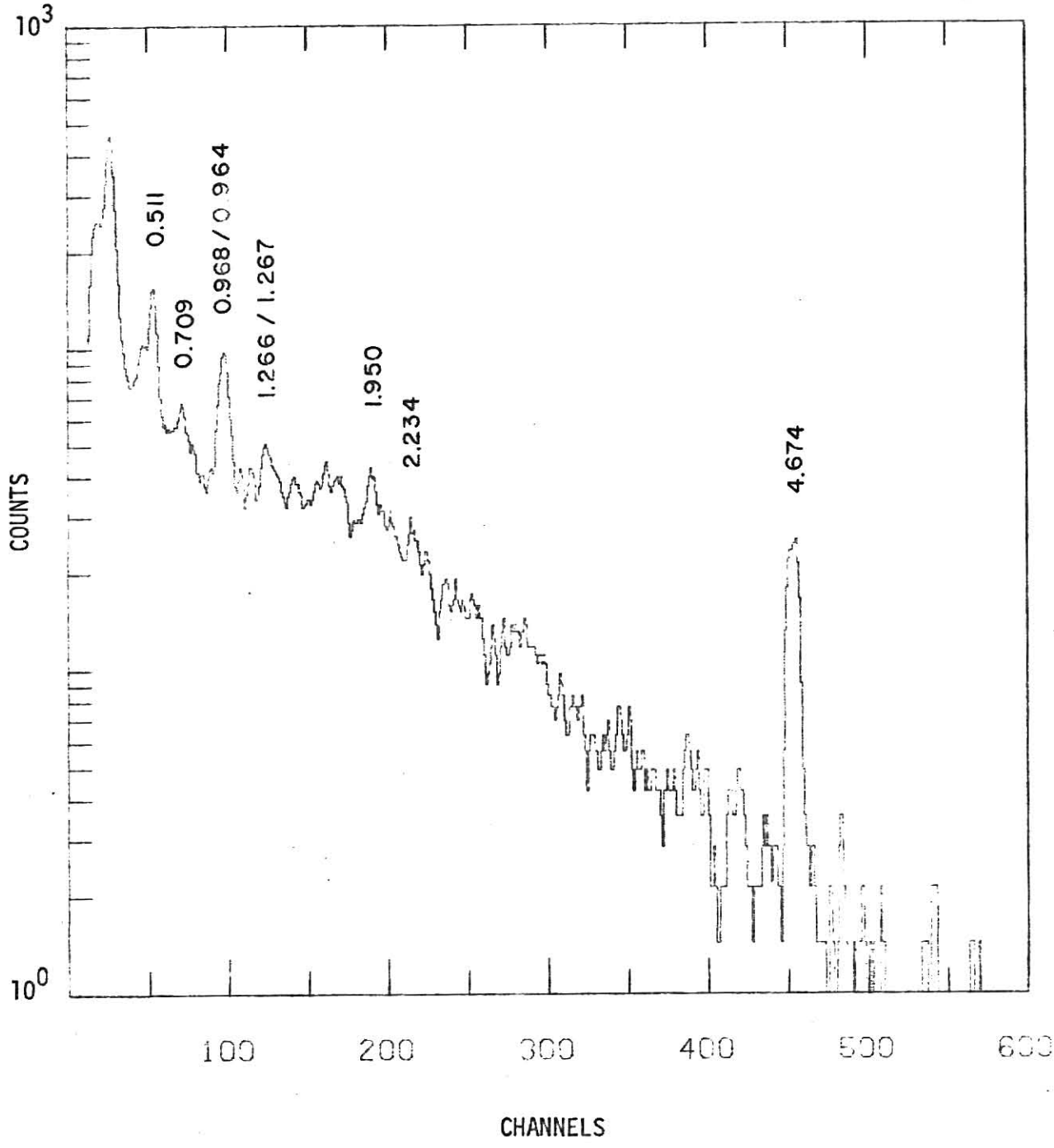

FIGURE 12

Figure 12 shows the coincidence gamma rays to the 1.976 MeV transition in P^{30} and the 1.957 MeV transition in P^{31}.

FIGURE 13

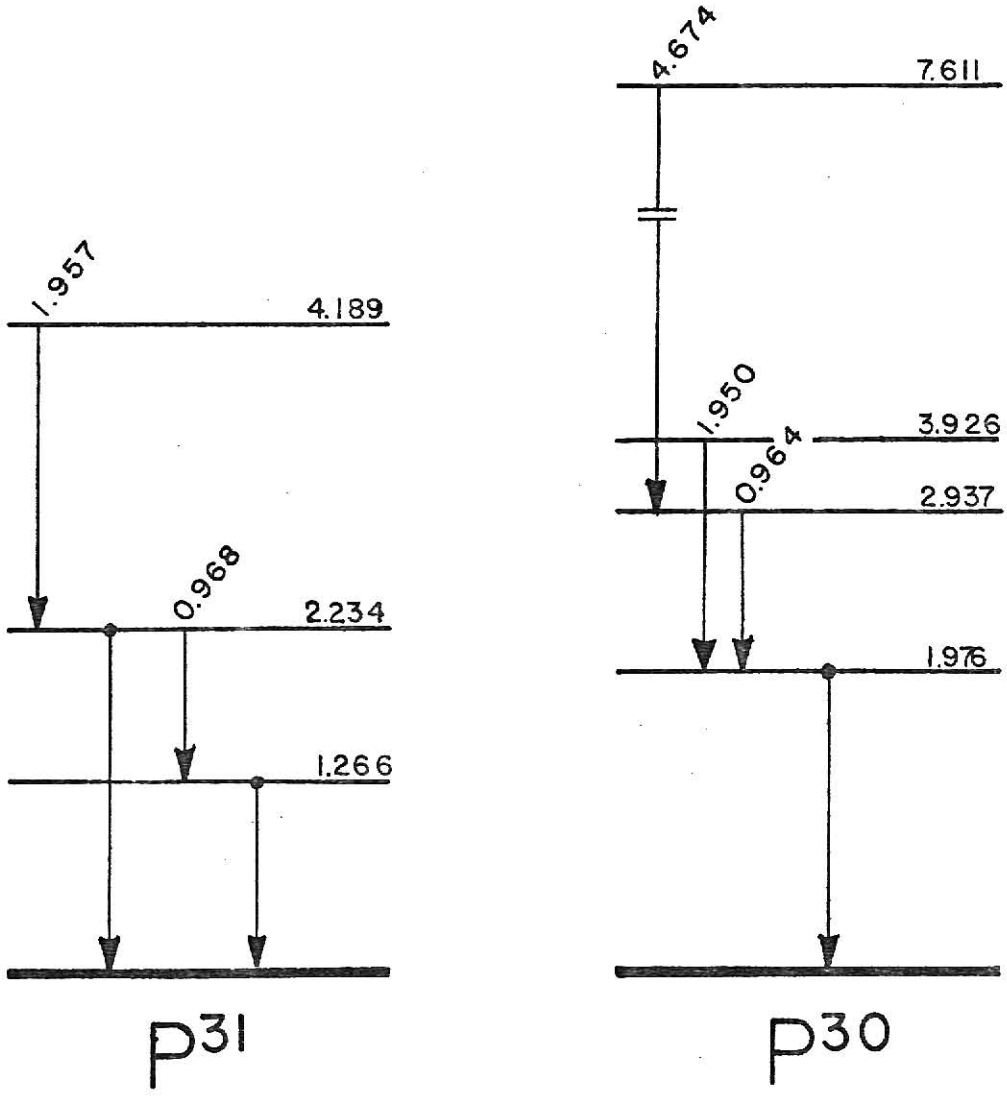

Figure 13 shows the parts of the level diagrams and the transitions of P^{31} and P^{30} which contribute to the spectrum in Figure 12.

4.3 Reactions with Chlorine

In the spectra taken with the thin NaCl target, no gamma rays were found which could certainly be related to a reaction with Cl. Since it was suspected, that those lines might be hidden by strong lines from reactions with Na^{23}, the gamma-gamma coincidence spectrum of a thick $BaCl_2$ target was taken in the same way as described for the NaBr target in the preceeding chapter. The total coincidence gamma spectrum is shown in Figure 14. The peak a was identified to belong to the ground state transition of the first excited level in Ti^{47} at 0.1588 MeV ((7) Page 317). The coincidence spectrum to this peak in Figure 15 shows the difference gamma rays to the first level from the next three states at 1.247, 1.442, 1.549 MeV and from the 2.414 MeV state. This ensures a $Cl^{37}(C^{12},d)\ Ti^{47}$ reaction. The theoretically possible $Cl^{35}(C^{12},\beta+)Ti^{47}$ reaction is not favored because of angular momentum matching conditions as explained in Chapter 2.1.

Efforts to identify the peaks b, c, and d in Figure 14 at 0.892, 1.228 and 1.526 MeV failed so far, although the coincidence spectra of these peaks showed strong gamma rays at 2.04, 2.87 and 3.6 MeV respectively. This was partly due to a lack of reliable recent level schemes for nuclei around Sc^{43}. Several peaks in the coincidence spectrum of peak b are consistent with known Sc^{45} energy levels.

It can be concluded, that chlorine is a promising target for a heavy ion reaction with C^{12}, which needs more investigation.

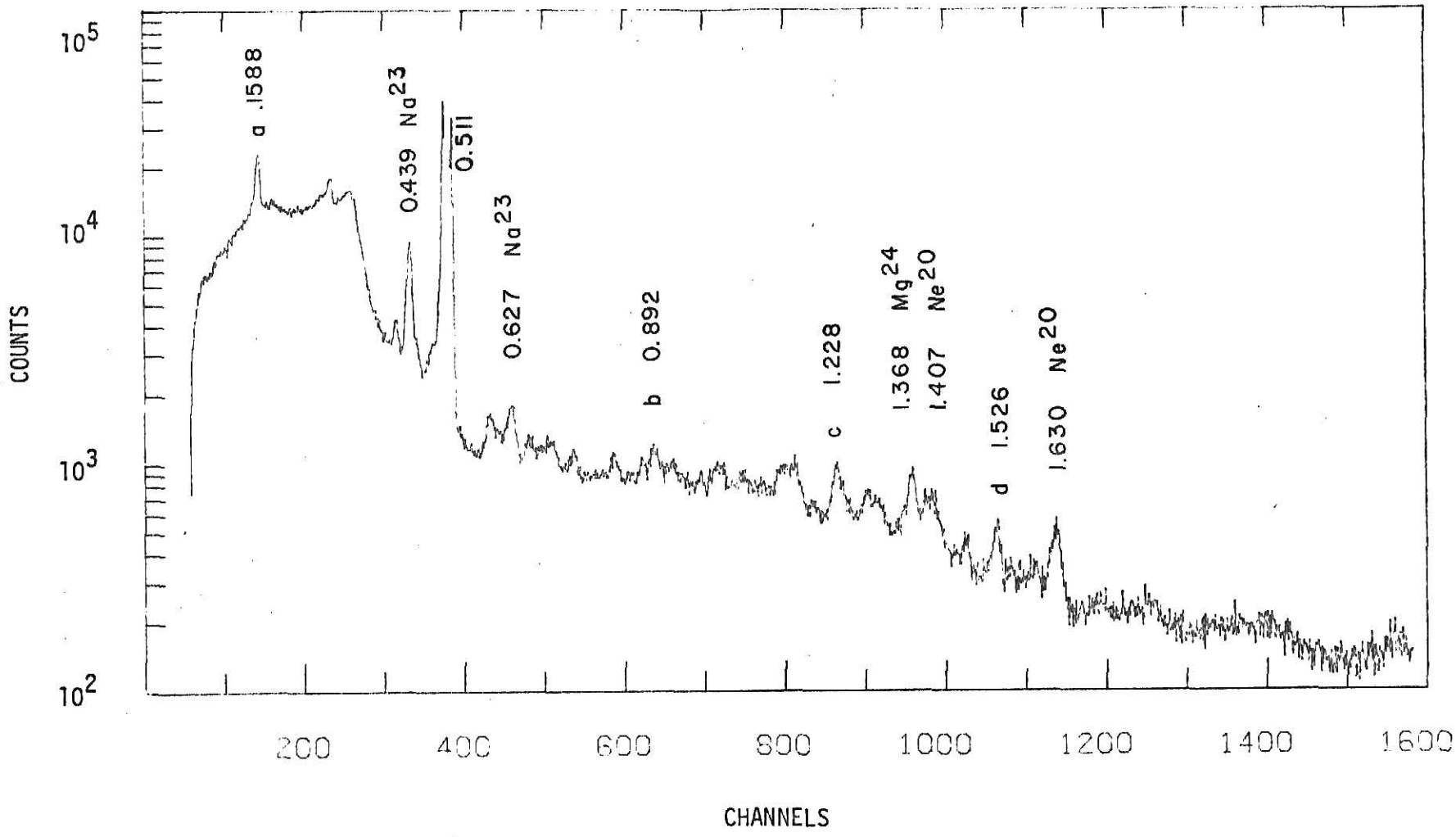

FIGURE 14 Total gamma ray coincidence spectrum from $BaCl_2$ target. Taken with Ge(Li) detector.

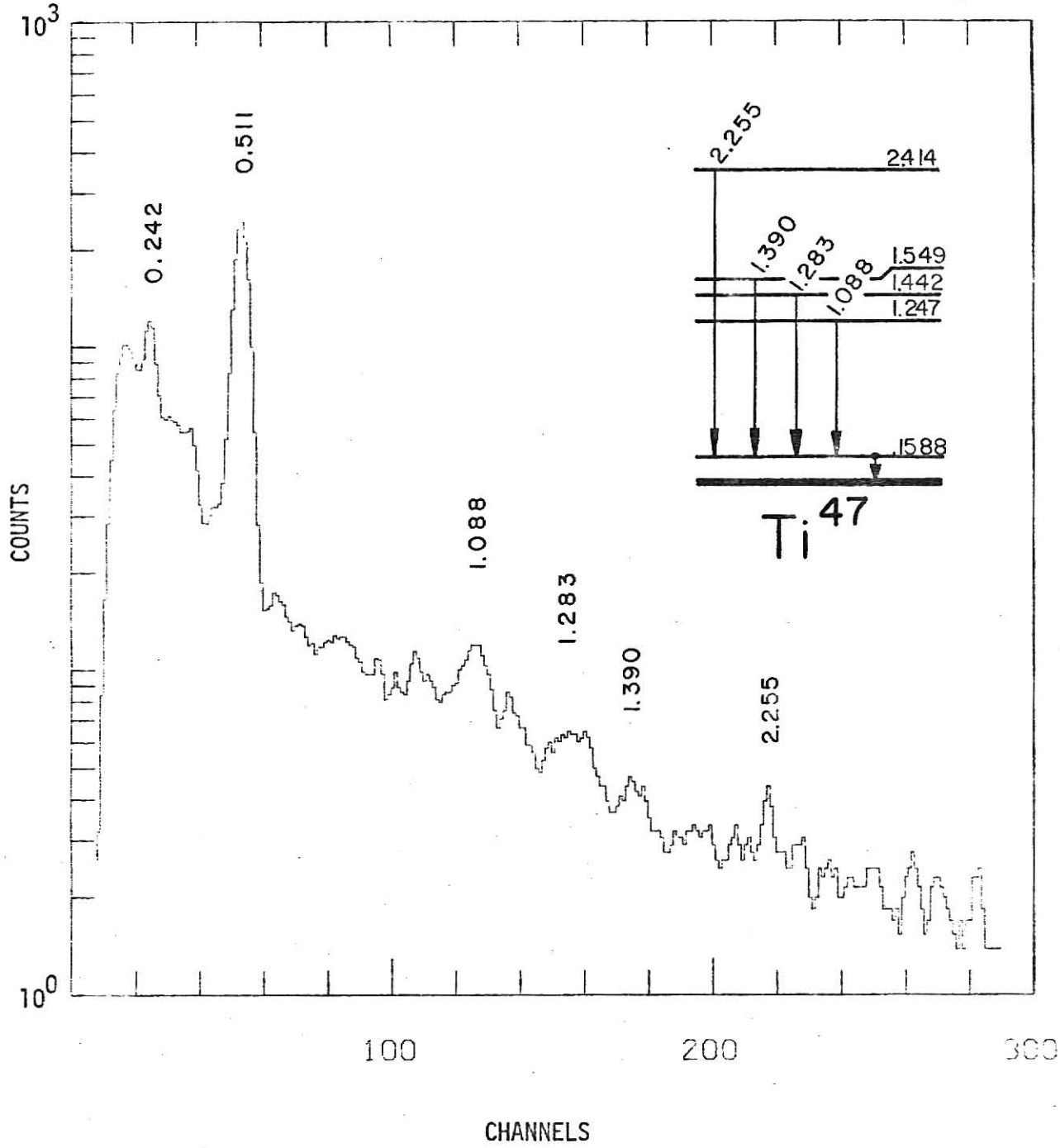

FIGURE 15

Figure 15 shows the gamma rays in coincidence with the 0.1588 MeV transition in Ti^{47}.

ACKNOWLEDGEMENTS

I wish to express my sincere thanks to Dr. Jim Legg, my major professor, for his constant help and guidance in performing the experiments for this project and for his assistance in writing this thesis.

Dr. Greg Seaman and Dr. Larry Weaver were kind enough to serve on my advisory committee.

My appreciation goes also to Joe Gray and Wolfram Hartwig, who assisted in collecting data and who provided together with Hugh Irvine computer programs for the data analysis. The spectra were plotted with programs from Clifford Woods and Helmut Laumer.

Finally, I want to thank G. Hartnell, B. Kraus, and their staff for keeping the PDP Computer and the 6 MV Tandem Van De Graaff Accelerator in working condition, and I am grateful to all the members of the Physics Department who helped to make my stay here a success.

REFERENCES

(1) P. Marmier and E. Sheldon
Physics of Nuclei and Particles
Academic Press, New York and London, 1969

(2) J. M. Blatt and V. F. Weisskopf
Theoretical Nuclear Physics
J. Wiley & Sons, New York, 1962

(3) A. E. Litherland and A. J. Ferguson
Gamma-Ray Angular Correlations from Aligned Nuclei Produced by Nuclear Reactions
Canadian Journal of Physics, 39 (1961) 788

(4) T. Mayer Kuckuk
Physik der Atomkerne
B. G. Teubner, Stuttgart, 1970

(5) J. B. Marion and F. C. Young
Nuclear Reaction Analysis
North Holland Publishing Co., Amsterdam, 1968

(6) A. E. Litherland
The Interpretation of Angular Distributions and Angular Correlations from the Reaction C^{12} (C^{12}, α γ) Ne^{20}
Canadian Journal of Science, 39 (1961) 1245

(7) Nuclear Data Group
Nuclear Data Sheets, Section B, No. 3-4
Oak Ridge, Tennessee, July 1970

(8) P. M. Endt and C. van der Leun
Energy Levels of Light Nuclei
Nuclear Physics A 105, Dec. 1967
North Holland Publishing Co., Amsterdam

GAMMA RAYS FROM VARIOUS (C^{12}, X) REACTIONS

by

ERICH WILHELM DREYER

Vordiplom, Justus Liebig Universitat, Giessen, Germany, 1970

AN ABSTRACT OF A MASTER'S THESIS

submitted in partial fulfillment of the

requirements for the degree

MASTER OF SCIENCE

Department of Physics

KANSAS STATE UNIVERSITY
Manhattan, Kansas

1973

ABSTRACT

A survey over several targets with $20 \leq A \leq 40$ was done , to observe possible $X(C^{12},d)Y$ reactions. The energy of the C^{12} beam was between 24 and 31.2 MeV and its charge state 4+ and 5+. Thin targets were Na, Cl, Si, S, and K. Only the Si target was enriched in Si^{28}, the others had natural abundance of isotopes. The experiment was set up according to the Litherland and Ferguson Geometry No. II.

It was found that the cross section was low for Si, S, and K. The negative result for S could come from its low evaporation point, which caused the S layer of the target to vanish during the experiment. The spectra for Si, S, and K were seriously disturbed by reactions with impurities of O^{16} and C^{12}, causing strong gamma rays from Ne^{20}, Na^{23}, Mg^{23}, and Mg^{24}. The NaCl target showed evidence for the wanted reaction. To distinguish contributions from reactions with Na and Cl and to obtain knowledge about the decay scheme of the respective residual nucleus, a second series of gamma gamma coincidence measurements with thick NaBr and $BaCl_2$ targets was performed. A higher beam energy of 31.2 MeV helped to increase the cross section for the wanted reaction and to keep the background down. Two dimensional spectra with pulses from a Ge(Li) and a NaI detector were taken and analysed.

It was found that the reactions $Cl^{37}(C^{12},d)Ti^{47}$, $Na^{23}(C^{12},\alpha)P^{31}$, and $Na^{23}(C^{12},\alpha n)P^{30}$ took place. Decay schemes were found by coincidence methods. Not all of the gamma rays of the chlorine spectrum have been identified. Further studies are suggested for this target.